FASTC-ID(RS)T-0099-93

(2)

FOREIGN AEROSPACE SCIENCE AND TECHNOLOGY CENTER

SPATIAL DISTRIBUTION OF THE THRESHOLD BEAM SPOTS OF LASER WEAPONS SIMULATORS

by

Qiwan Fang, Xaohui Zhang

HUMAN TRANSLATION

FASTC-ID(RS)T-0099-93 8 September 1993

MICROFICHE NR: 93C000537

SPATIAL DISTRIBUTION OF THE THRESHOLD BEAM SPOTS OF LASER WEAPONS SIMULATORS

By: Qiwan Fang, Xaohui Zhang

English pages: 17

Source: Chinese Journal of Lasers, Vol. 19, No. 5, 1992; pp. 363-370

Country of origin: China
Translated by: SCITRAN
F33657-84-D-0165
Requester: FASTC/TATD/Bruce Armstrong

THIS TRANSLATION IS A RENDITION OF THE ORIGINAL FOREIGN TEXT WITHOUT ANY ANALYTICAL OR EDITORIAL COMMENT STATEMENTS OR THEORIES ADVOCATED OR IMPLIED ARE THOSE OF THE SOURCE AND DO NOT NECESSARILY REFLECT THE POSITION OR OPINION OF THE FOREIGN AEROSPACE SCIENCE AND TECHNOLOGY CENTER.	PREPARED BY: TRANSLATION DIVISION FOREIGN AEROSPACE SCIENCE AND TECHNOLOGY CENTER WPAFB, OHIO

GRAPHICS DISCLAIMER

All figures, graphics, tables, equations, etc. merged into this translation were extracted from the best quality copy available.

Job# FASTC-ID(RS)T-0099-93 (517-370)

Chinese Journal of Lasers, Vol. 19, No. 5, May 1992
Edited by Chinese Optical Society
Published by Science Publishing Co.

SPATIAL DISTRIBUTION OF THE THRESHOLD BEAM SPOTS OF LASER WEAPONS SIMULATORS[1]

/363*

By Qiwan Fang and Xaohui Zhang

(Naval Academy of Engineering, No. 505 Lab., Wuhan 430033)

ABSTRACT

This paper was based on the transmission theory of elliptical Gaussian beam fluxes in deriving some transmission equations for the threshold beam spots of laser weapon simulators, in order to revise and expand the expressions for the threshold beam spots, their maximum range, the extinction function and the irradiance in ADA 102276, and also in this paper, verification tests were carried out.

1. INTRODUCTION

Laser weapon simulators are being used as military training equipment, using beams in place of bullets and simulating all sorts of weapons in recreating their weapon effectiveness, and they can also simulate different services of the armed forces in carrying out battle station exercises for the combined weapons systems; they are breaking up the old tradition of real target practice and tactical maneuvers, saving the expenses on bullets, reducing

---

[1] Date of receiving the drafted copy: March 14, 1990; Date of receiving the revised drafted copy: June 4, 1990.

* Numbers in margins indicate foreign pagination. Commas in numbers indicate decimals.

equipment wear, but at the same time they are realistic, eliminating the vulnerable factors in the judgements of the judges, raising the quality of troop training, and saving a lot of military expense. Since the middle of the 70's, they have already established a number of systematic products, equipped the armed forces of more than 100 countries around the world, and they can simulate cannon fodder, guided missiles, rockets, bullets, etc. for 36 kinds of weapons systems.

To simulate the weapon ranges and the spread of bullets in order to guarantee the effective casualty ratio with respect to the distance as compared to the actual weapons, one has to study the transmission characteristics of the threshold beam spots of these weapon simulators; a number of authoritative research results from here and abroad can be found in the Literature [1], but the precondition in all these studies was in assuming that the Gaussian beam flux was a circular one. In reality, the transmitted Gaussian beam fluxes from the simulators here and abroad were elliptic and the ellipticity sometimes could be quite prominent. This paper attempts to develop a theory of elliptic Gaussian beam fluxes[2,3] to revise and expand the transmission equations which appeared in the Literature [1], and to carry out the tests to verify them.

2. THEORETICAL ANALYSIS

The relationship between the transmission efficiency of the laser weapon simulators and their irradiance is shown by

$$P_0 = \int_{A(z)} H(x, y, z)\, dA(z) \tag{1}$$

where A(z) and dA(z) are, respectively, the irradiated area and the irradiated area-element at the location of z. As the actual light source of the simulators, here and abroad one usually uses a semiconductor lasing apparatus, formed by the emission optical antennae and some simple transparent mirrors; when the elliptic Gaussian beam flux is transported from the semiconductor laser, it is transformed through the transparent mirror, but it remains as an elliptical Gaussian beam flux, and thus the irradiance function of the simulator in the plane perpendicular to the optic axis z is in an elliptic Gaussian form. Consequently by solving the wave equation with the Lamber theorem, one gets

$$H(x, y, z) = H_0 \frac{\omega_{0x}\omega_{0y}}{\omega_x(z)\omega_y(z)} \exp\left[-\frac{2x^2}{\omega_x^2(z)} - \frac{2y^2}{\omega_y^2(z)} - \alpha z\right] \quad (2)$$

where H_0 is the maximum central irradiance at $x = y = z = 0$; ω_{0x}, ω_{0y} and $\omega_x(z)$, $\omega_y(z)$ are, respectively, the flux in the x and y direction, and the long and short radii of the beam spot at z; α is the air attenuation coefficient. Since at $z = 0$, the area of the beam spot $A(0) = \pi\omega_x(0)\omega_y(0)$, Eqn.(1) becomes

$$P_0 = \int_{A(0)} \frac{H_0\omega_{0x}\omega_{0y}}{\omega_x(0)\omega_y(0)} \exp\left[-\frac{2x^2}{\omega_x^2(0)} - \frac{2y^2}{\omega_y^2(0)}\right] dA(0)$$

When the perpendicular coordinate system is transformed to the polar coordinate system, with a little manipulation one gets

$$P_0 = (1-e^{-2}) H_0\omega_{0x}\omega_{0y}\int_0^{\pi/2} \frac{\omega_x(0)\omega_y(0)d\theta}{\omega_y^2(0)\cos^2\theta + \omega_x^2(0)\sin^2\theta} = \frac{e^2-1}{2e^2}\pi\omega_{0x}\omega_{0y}H_0 \quad (3)$$
$$H_0 = 0.73626 P_0/(\omega_{0x}\omega_{0y})$$

By substituting it into Eqn.(2), one gets the spatial distribution of the irradiance of the simulators:

$$H(x,y,z) = \frac{0.73626\, P_0}{\omega_x(z)\omega_y(z)} \exp\left[-\frac{2x^2}{\omega_x^2(z)} - \frac{2y^2}{\omega_y^2(z)} - \alpha z\right]$$

If the long-distance dissipation angles are, respectively, θ_x and θ_y in the x- and y-direction when the laser is in the x-z and y-z plane, the image spread would be 2ρ, assuming the simulated range to be at a distant field, because of

$$\omega_x(z)=\theta_x(z-\rho),\ \omega_y(z)=\theta_y(z+\rho) \tag{4}$$

that is,

$$H(x,y,z)=\frac{0.73626\,P_0}{\theta_x\theta_y(z^2-\rho^2)}\exp\left[-\frac{2x^2}{\theta_x^2(z-\rho)^2}-\frac{2y^2}{\theta_y^2(z+\rho)^2}-\alpha z\right] \tag{5}$$

If the threshold irradiance of the detector is T, then at H(x,y,z) = T the detector can function normally. The threshold beam spot of the simulator is defined when the transmitted irradiance of the simulator is equal to some beam spot within the range of the threshold irradiance of the detector. The boundary equation of the threshold beam spot is

$$\frac{0.73626\,P_0}{\theta_x\theta_y(z^2-\rho^2)}\exp\left[-\frac{2x^2}{\theta_x^2(z-\rho)^2}-\frac{2y^2}{\theta_y^2(z+\rho)^2}-\alpha z\right]=T$$

if

$$L=\sqrt{0.73626\,P_0/T}=0.8581\sqrt{P_0/T},\ \ \theta=\sqrt{\theta_x\theta_y} \tag{6}$$

because of

$$\frac{x^2}{\frac{1}{2}\theta_x^2(z-\rho)^2\left[\ln\frac{L^2}{\theta^2(z^2-\rho^2)}-\alpha z\right]}+\frac{y^2}{\frac{1}{2}\theta_y^2(z+\rho)^2\left[\ln\frac{L^2}{\theta^2(z^2-\rho^2)}-\alpha z\right]}=1 \tag{7}$$

where L is called the characteristic length. From Eqn.(7), one knows that the distribution of the threshold beam spot which coincides with the normally defined beam spot in the cross-sectional plane perpendicular to the optical axis is elliptic. If the long and short axes of the ellipse of the beam spot are, respectively, $\omega_{Tx}(z)$ and $\omega_{Ty}(z)$, then from Eqn. (7), one has

$$\omega_{Tx}(z)=\frac{\theta_x}{\sqrt{2}}(z-\rho)\left[\ln\frac{L^2}{\theta^2(z^2-\rho^2)}-\alpha z\right]^{1/2} \tag{8}$$

and

$$\omega_{Ty}(z)=\frac{\theta_y}{\sqrt{2}}(z+\rho)\left[\ln\frac{L^2}{\theta^2(z^2-\rho^2)}-\alpha z\right]^{1/2} \tag{9}$$

Thus as can be seen by comparing the above two equations with Eqn. (6), the distinction of the threshold beam spot from the ordinary beam spot is as follows: The long and short axes are not some monotonic functions of z, but as z increases they increase with it initially but decline soon afterwards, finally to reach zero. If their maximum values are, respectively, at z_x^* and z_y^*; that is, $\omega_{Tx}(z)$ and $\omega_{Ty}(z)$ yield their derivatives at z_x^* and z_y^* to be, respectively, $\omega'_{Tx}(z_x^*) = 0$ and $\omega'_{Ty}(z_y^*) = 0$, they can be solved from the above two equations to be

$$z_x^* = \frac{L}{\theta}\left[\exp\left(-\frac{z_x^*}{z_x^*+\rho} - \frac{3}{2}\alpha z_x^* + \frac{\alpha}{2}\rho\right) + \rho^2\right]^{1/2} \tag{10}$$

$$z_y^* = \frac{L}{\theta}\left[\exp\left(-\frac{z_y^*}{z_y^*-\rho} - \frac{3}{2}\alpha z_y^* + \frac{\alpha}{2}\rho\right) + \rho^2\right]^{1/2} \tag{11}$$

and when the above two equations are, respectively, substituted into Eqns. (8) and (9), one just gets the maximum radii of the threshold beam spot,

$$\omega_{Txm} = \frac{\theta_x}{\sqrt{2}}(z_x^* - \rho)\sqrt{\frac{z_x^*}{z_x^*+\rho} + \frac{1}{2}\alpha(z_x^* - \rho)} \tag{12}$$

$$\omega_{Tym} = \frac{\theta_y}{\sqrt{2}}(z_y^* + \rho)\sqrt{\frac{z_y^*}{z_y^*+\rho} + \frac{1}{2}\alpha(z_y^* - \rho)} \tag{13}$$

At the point zm for the threshold beam spot it reaches the maximum range; that is, at the location of z_m, $A(z_m) = \pi\omega_{Tx}(z_m)\omega_{Ty} \cdot (z_m) = 0$ and by substituting into Eqns. (8) and (9), one immediately finds the maximum range

$$z_m = \sqrt{\frac{L^2}{\theta^2} e^{-\alpha z_m} + \rho^2} \tag{14}$$

3. SIMPLIFICATION OF THE EQUATIONS AND THE SOLUTIONS BY ITERATION

The image spread from the Gaussian beam flux transmitted from a semiconductor laser is smaller than the simulated range by approximately 3 orders of magnitude, and thus it can be approximated by $z + p \approx z - p \approx z$; that is, both Eqns. (6) and (8) can be simplified to be

$$H(x, y, z) = \left(\frac{L}{\theta z}\right)^2 \exp\left[-\frac{2x^2}{\theta_x^2 z^2} - \frac{2y^2}{\theta_y^2 z^2} - \alpha z\right] \tag{15}$$

$$\omega_{Tx}(z) = \frac{\theta_x}{\sqrt{2}} z \left[2 \ln \frac{L}{\theta z} - \alpha z\right]^{1/2} \tag{16}$$

$$\omega_{Ty}(z) = \frac{\theta_y}{\theta_x} \omega_{Tx}(z) \tag{17}$$

$$z^* = z_x^* = z_y^* = \frac{L}{\theta \sqrt{e}} \exp\left(-\frac{3}{4} \alpha z^*\right) \tag{18}$$

$$\omega_{Txm} = \sqrt{\frac{\theta_x}{2\theta_y}}\, L \sqrt{1 + \frac{1}{2} \alpha z^*}\, \exp\left(-\frac{1}{2} - \frac{3}{4} \alpha z^*\right) \tag{19}$$

$$\omega_{Tym} = \frac{\theta_y}{\theta_x} \omega_{Txm} \tag{20}$$

$$z_m = \frac{L}{\theta} \exp\left(-\frac{1}{2} \alpha z_m\right) = 0.8581 \sqrt{\frac{P_0}{T\theta_x\theta_y}}\, \exp\left(-\frac{1}{2} \alpha z_m\right) \tag{21}$$

$$\frac{z^*}{z_m} = \frac{1}{\sqrt{e}} \exp\left(-\frac{1}{2} \alpha z_m - \frac{3}{4} \alpha z^*\right) \tag{22}$$

In vacuum or in some rapidly dropping atmosphere, the maximum range, the radii of threshold beam spot and the maximum theoretical value for z^* can all be found from the above mentioned equations to be

$$z_{m0} = \frac{L}{\theta} = 0.8581 \sqrt{\frac{P_0}{T\theta_x\theta_y}} \tag{23}$$

$$\omega_{Txm0} = \sqrt{\frac{\theta_x}{2e\theta_y}}\, L = 0.368 \sqrt{\frac{\theta_x P_0}{\theta_y T}} \tag{24}$$

$$\omega_{Tym0} = \frac{\theta_y}{\theta_x} \omega_{Txm0} \tag{25}$$

$$z_0^* = z_{x0}^* = z_{y0}^* = \frac{L}{\theta \sqrt{e}} = \frac{1}{\sqrt{e}} z_{m0} = 0.6065 z_{m0} \tag{26}$$

The maximum range Eqn.(21) and the threshold beam spot Eqn.(18) both are transcendental equations, which can be solved by iterations: By taking Eqns. (23) and (26) at α = 0 as their initial approximations and then by use of

$$z_{m,n+1}=\frac{L}{\theta}\exp\left(-\frac{1}{2}\alpha z_{m,n}\right) \quad n=0,\ 1,\ 2\cdots \tag{27}$$

$$z^{*}_{n+1}=\frac{L}{\theta\sqrt{e}}\exp\left(-\frac{3}{4}\alpha z^{*}_{n}\right) \quad n=0,\ 1,\ 2\cdots \tag{28}$$

respectively, we find the needed z_m and z^*. The reiterative number n should satisfy the corresponding degree of accuracy. When the solution by iteration is carried out in the standard air (α = 0.12 km^{-1}), the maximum ranges of the following two kinds of simulators of λ = 904 nm are as follows:

(1) For America's MILES VES, P_o = 1.95 W, T = 7 x 10^{-6} W/cm^2, θ = 1.2 mrad

(2) For China's Naval chaser gun laser simulator, P_o = 2.8 W, T = 2 x 10^{-5} W/cm^2, θ_x = 0.8 mrad, θ_y = 0.18 mrad.

Here calculations have been carried out up to the errors of less than one thousandth as shown in Table 1.

Table 1 Iterative process of the maximum range (unit: m)

Nation	Name	z_{m0}	z_{m1}	z_{m2}	z_{m3}	z_{m4}	z_{m5}	z_{m6}	z_{m7}	z_{m8}	z_{m9}
U.S.	MILES VES	3774	3009	3151	3124	3129	3128				
China	Chaser simulator	8460	5092	6233	5820	5966	5914	5933	5926	5929	5928

Thus z_m was obtained to be 3,128 m for the former, while it was 5,928 m for the latter. When the atmospheric drop became intense, z_m and z^* also declined monotonically, but the ratio of z^*/z_m rose smoothly in a monotonic fashion; by use of Eqns. (27) and (28) to make iteration, under various different visibility conditions to find z_m, z^* and z^*/z_m for our national naval chaser laser simulators, the results are shown in Table 2.

Table 2. z_m. z^* and z^*/z_m of laser simulator versus visibility

V (km)	∞	60	40	23.5	15	10	8	5	4	3
$\alpha(km^{-1})$	0	0.047	0.072	0.13	0.19	0.29	0.36	0.57	0.71	0.96
z_m (m)	8460	7151	6657	5928	5174	4442	4068	3301	2959	2521
z^* (m)	5131	4394	4109	3683	3235	2794	2566	2095	1883	1610
z^*/z_m	0.6065	0.6144	0.6172	0.6213	0.6252	0.6290	0.6308	0.6347	0.6364	0.6386

4. DISTRIBUTION OF THRESHOLD BEAM SPOTS AND THE EXTINCTION FUNCTION

The effective casualty range of some realistic simulator weapons, and the relationship between the threshold beam spot and the change of the distance are parallel to the casualty probability of the simulating weapons. Consequently except beyond the maximum range and beyond the range of maximum threshold beam spots, the spatial shape of threshold beam spot and the maximum length of the radii are the important characteristic coefficient of a simulator. The spatial distribution of the threshold beam spots can be calculated with Eqns. (16) and (17), and the calculation was made on the naval chaser cannon laser simulators for two kinds of visabilities and the results are shown in Table 3.

Table 3 Spatial distribution of threshold beam spot of laser chaser simulator

V(km	(km^{-1})	Half axes of threshold term	z(m)														
			200	500	1000	1250	1500	1750	2000	2300	2500	3000	3300	3600	4000	4400	5000
5	0.57	ω_{Tx}	0.307	0.655	1.088	1.247	1.369	1.454	1.494	1.480	1.423	1.025	0.080				
		ω_{Ty}	0.069	0.147	0.245	0.281	0.308	0.327	0.336	0.333	0.290	0.230	0.018				
10	0.29	ω_{Tx}	0.308	0.664	1.128	1.315	1.476	1.606	1.717	1.811	1.851	1.861	1.796	1.660	1.316	0.442	
		ω_{Ty}	0.069	0.149	0.254	0.296	0.332	0.362	0.386	0.407	0.416	0.417	0.404	0.374	0.296	0.099	
23.5	0.12	ω_{Tx}	0.309	0.669	1.152	1.355	1.536	1.698	1.84	1.985	2.065	2.221	2.276	2.453	2.288	2.197	1.901
		ω_{Ty}	0.070	0.151	0.258	0.305	0.346	0.382	0.414	0.447	0.465	0.500	0.512	0.552	0.514	0.494	0.428

As it can be seen in Eqns. (19) and (20), the maximum radial lengths of the threshold beam spots are the same as z_m and z^*. They showed the maximum values in vacuum, but they declined monotonically as α increased; such laser was receiving some attenuation phenomena during the transmission in air and it is called the effect of extinction. Although α can describe the extinction attenuation in terms of z_m, z^*, z^*/z_m and ω_{Txm}, etc., yet the relationship between wTxm and α is most complex. This is because z^* in Eqn. (19) is to be determined by the transcendental equation which has a bearing on α. For simplicity, reference [1] introduced the extinction coefficient $J = \frac{1}{4}\alpha z^*$ and extinction function $F(J)$, where $F(J)$ was defined as the ratio between the maximum radial length of the threshold beam spot in air and the maximum radial length in vacuum; that is,

$$F(J)=\omega_{Txm}/\omega_{Txm0} \quad (29)$$

with $J = \frac{1}{4}\alpha z^*$ and with Eqns. (19), (24) and (29) one can get

$$F(J)=\sqrt{1+J}/\exp(1.5J) \quad (30)$$

Reference [1] estimated the final form of the extinction coefficient of the extinction effect in determining the air attenuation as J/dL/4θ, but the present authors believe it to be inappropriate. Although this equation allows J to take L/2θ as the final substitution for z* in the definition, because L/2θ = 1/2 z_{m0} is one half of the maximum range in vacuum, it is related to the atmospheric attenuation, and thus it is a constant for each of the simulators; furthermore, z* is the range of the maximum threshold beam spot in air, and it is a function which is related to the atmospheric attenuation coefficient α, and thus these two cannot be identical, nor can be approximated to each other. Hence this paper attempts to make the following modification: To develop Eqn. (18) in terms of power series approximation values, at the same time by use of Eqn. (23) with some adjustments, one can determine the key parameter group J of the atmospheric extinction effect as follows:

$$J=\frac{1}{4}\alpha z_{m0}\exp\left(-\frac{\alpha z_{m0}}{2+\alpha z_{m0}}\right)$$

$$=0.2145\alpha\sqrt{\frac{P_0}{T\theta_x\theta_y}}\exp\left(-\frac{0.8581\alpha\sqrt{\frac{P_0}{T\theta_x\theta_y}}}{2+0.8581\alpha\sqrt{\frac{P_0}{T\theta_x\theta_y}}}\right) \tag{31}$$

From Eqns. (29), (19), (20) and (6), one can get the maximum radial length of the threshold beam spot of the simulator under various atmospheric visibility conditions to be

$$\omega_{Txm}=0.368\sqrt{\frac{\theta_x P_0}{\theta_y T}}\,F(J) \tag{32}$$

$$\omega_{Tym}=0.368\sqrt{\frac{\theta_y P_0}{\theta_x T}}\,F(J)=\frac{\theta_y}{\theta_x}\,\omega_{Txm} \tag{33}$$

Since P_0, T, θ_x and θ_y of the above-mentioned naval chaser gun laser simulator are known, one can calculate the maximum radial lengths of threshold beam spots with Eqns. (24) and (25) to be ω_{Txm0} = 2.903 m and ω_{Tym0} = 0.653 m, and for the maximum radii under various atmospheric visibility conditions, one can use Eqn. (31) to find J, Eqn. (30) to determine F(J), and then reuse the values obtained for the above two equations; on the other hand one also uses formulas of reference [1] to make similar calculations. Now these two kinds of results are shown in Table 4. By comparing these two kinds one can see: Reference [1] used constant 1/2 z_{m0} for z* which was a function of α, assuming $J \propto \alpha$; this means that as α increased, J increased too rapidly, while F decelerated; the attenuation of the threshold beam spot is intensified, especially in weather in which α is relatively large; the situation appeared to be more severe than it should be, and thus the equation for J ought to be revised to become Eqn.(31).

Table 4 The comparison of two kinds of calculated results of extinction function and the maximum axes

	V (km)	∞	60	40	23.5	15	10	8	5	4	3
	α (km^{-1})	0	0.047	0.072	0.12	0.19	0.29	0.36	0.57	0.71	0.96
J	By equation α/4 z_{m0} of ref. [1]	0	0.1988	0.3046	0.5076	0.8037	1.2267	1.5228	2.4111	3.0033	[illegible].0608
	By equation (31) of this text	0	0.0842	0.1206	0.1812	0.2574	0.3536	0.4164	0.5964	0.7092	[illegible]7101
$F(J)$	By equation of ref. [1]	1.000	0.8059	0.7233	0.5734	0.4028	0.2370	0.1618	0.0496	0.0221	0.[illegible]
	By equation (30) of this text	1.000	0.9177	0.8834	0.8281	0.7622	0.6845	0.6378	0.5176	0.4512	0.3529
Δr_{Tm} (m)	By equation of ref. [1]	2.903	2.340	2.100	1.665	1.168	0.688	0.470	0.144	0.064	0.015
	By equation(32) of this text	2.903	2.664	2.565	2.404	2.213	1.987	1.850	1.508	1.310	1.0[illegible]
Δr_{Ym} (m)	By equation of ref. [1]	0.653	0.526	0.472	0.374	0.263	0.155	0.106	0.032	0.014	0.003
	By equation(33) of this text	0.653	0.599	0.577	0.541	0.498	0.447	0.416	0.338	0.295	0.230

The characteristic parameters for the above mentioned naval chaser gun simulator and the values calculated in this paper, as related to visibility, are shown in Fig. 1.

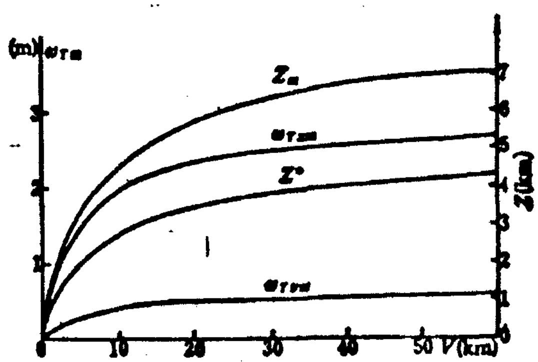

Fig. 1 Characteristic parameters of laser chaser simulator versus visibility

5. EXPERIMENTAL RESULTS

The spatial distribution of threshold beam spots of the above-mentioned laser chaser simulator was measured within the range of 2.3 km for the runway in a certain airfield, and its maximum range was also measured at the same time. The experimental results from the selected parts are shown in Tables 5 and 6. In Table 6, the maximum ranges obtained in this paper and those calculated in Reference [1] are shown. The beam spot diameter of the emission angle defined in reference [1] was in general set at the location where the illumination was 10% of the maximum illumination, and consequently, because reference [1] adopted circular Gaussian beam fluxes in computing the equations, the selection of emission angle θ' in the equation seemed to the present authors to be of the following two situations: I. Here and abroad they all use the horizontal emission angle, namely $\theta' = \theta'_x$ (because θ'_y is extremely small); II. The authors are ready to utilize reference [1] to approximate the elliptic Gaussian flux to a circular one, and by use of the root-mean-square of the mutually perpendicular emission angles as the average emission angle, namely $\theta' = \sqrt{\theta_x \theta_{y0}}$. Thus by so doing, this made the present paper more reasonable. Now the experimental values of the spatial distribution of the threshold beam spot and the theoretical calculation of this paper are shown in Figs. 2 and 3. From Figs. 2 and 3, and Tables 5 - 6, one can see that the theoretical calculation of the characteristic parameters of laser chaser simulator by use of the simplified transmission equation of this paper agrees basically well with the experimental values. It explains the accuracy of this modified equation of this paper for the threshold beam spots and extinction function, derived from the transmission theory of elliptic Gaussian beam flux.

Table 5 Tested results of distribution of threshold beam spot.

V (km)	α (km^{-1})	Half axes of threshold beam spot (m)	s(m)							
			200	500	1000	1250	1500	1750	2000	2300
5	0.57	$2\omega_{Tx}$	0.55	0.85	1.50	1.70	2.20	2.70	2.90	2.70
		$2\omega_{Ty}$	0.35	0.40	0.45	0.50	0.55	0.58	0.62	0.60
10	0.39	$2\omega_{Tx}$	0.60	1.10	1.80	2.30	2.50	2.80	3.30	3.70
		$2\omega_{Ty}$	0.40	0.50	0.58	0.60	0.64	0.66	0.70	0.75

Table 6 Experimental and calculated values of the maximum range

V (km)	$s_{m,exp}$ (m)	$s_{m,cal}$ (m)		
		By equation of ref. [1]		By equation (37) of this text
		I. $\theta' = \theta_e$	II. $\theta' = \sqrt{\theta_e \theta_v}$	
30	6090	3818	5014	6278
15	5190	2856	4910	5174

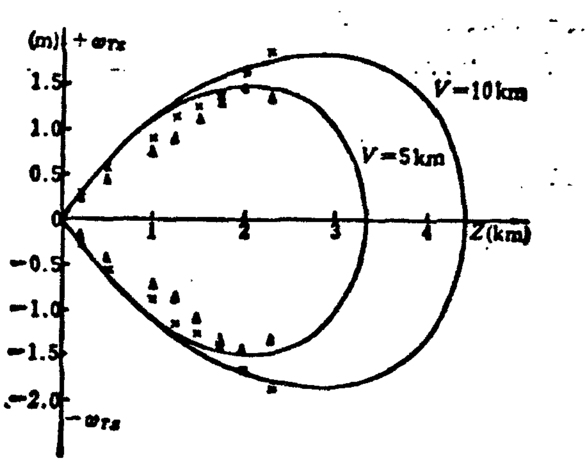

Fig. 2 $2\omega_{Tx}$ versus the range
- calculated theoretical curves
×-V = 10 km experimental points
▲-V = 5 km experimental points

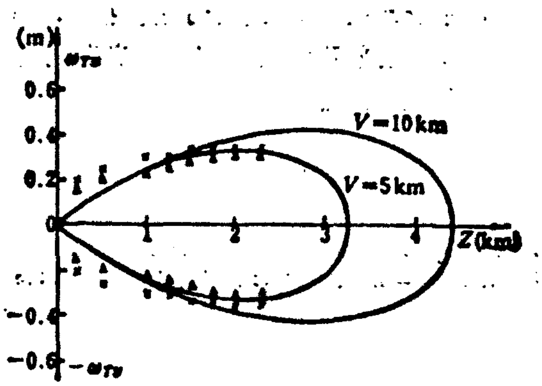

Fig. 3 $2\omega_{Ty}$ versus the range
- calculated theoretical curves
×-V = 10 km experimental points
▲-V = 5 km experimental points

6. CONCLUSION

1. The maximum radial lengths of the threshold beam spot of laser weapons simulator are directly proportionate to the laser transmission efficiency as well as the root-mean-square of the threshold irradiance ratio of the detector, and also directly proportionate to the root-mean-square value of the emission angles of the same direction and the perpendicular direction.

2. If the light source of the simulator is of a circular Gaussian flux ($\theta_x = \theta_y$), the maximum radius of the threshold beam flux is unaffected by the laser apparatus. However, for the elliptic Gaussian flux transmitted from a semiconductor laser instrument used here and abroad, because the maximum radial lengths are directly proportionate to the root-mean-square value of emission angles of the same

direction and of the perpendicular direction, one can adjust θ_x and θ_y by the design of antennae and by the parameters of the transparent mirror to vary the maximum radial lengths in the two mutually perpendicular directions for the threshold beam spot in satisfying the requirement of simulated weapons tactical capabilities.

3. The dependence of the maximum radial lengths of the threshold beam spot on the atmospheric attenuation to grow or to shrink is determined by extinction parameter J, while J itself depends on the transmission efficiency of the laser, emission angles in both directions, the threshold irradiance of the detector, and the attenuation coefficient of the air.

4. The maximum range is directly proportional to the root-mean-square value of the transmission efficiency of the laser and the threshold irradiance of the detector, but inversely proportional to the root-mean-square of the product of the mutually perpendicular emission angles.

5. The maximum range of the threshold beam spot and the maximum range itself are both depending on the atmospheric attenuation to rise or to fall, but the ratio of these two values rises only slowly; it is about 60% in the standard atmosphere, it is about 63% at V = 8 - 10 km, and in the visibility of 3 km of the chaser range (if it was below 3 km, the target was not visible) it is about 64%.

Prof. Ping-Yuan Ye provided some useful guidance for this paper; Z. Ye, Q. Wang, W. Cha, Z. Lee, T. Zhin, K. Lee and D. Chen shared useful assistance; M. Teng, S. Lieu, Z. Zhang, Y. Zhang, and other comrades took part in the airfield experimental works, and thus gratitude are sincerely expressed to them.

REFERENCES

1. ADA102276, Appendix B

2. A. Yariv, Optical Electronics, 1985, 47-50.

3. K. Gue, et al.: Laser Beam Optics, Beijing Institute of Technology Publishers, 1988.

DISTRIBUTION LIST

DISTRIBUTION DIRECT TO RECIPIENT

ORGANIZATION	MICROFICHE
B085 DIA/RTS-2FI	1
C509 BALLOC509 BALLISTIC RES LAB	1
C510 R&T LABS/AVEADCOM	1
C513 ARRADCOM	1
C535 AVRADCOM/TSARCOM	1
C539 TRASANA	1
Q592 FSTC	4
Q619 MSIC REDSTONE	1
Q008 NTIC	1
Q043 AFMIC-IS	1
E051 HQ USAF/INET	1
E404 AEDC/DOF	1
E408 AFWL	1
E410 ASDTC/IN	1
E411 ASD/FTD/TTIA	1
E429 SD/IND	1
P005 DOE/ISA/DDI	1
P050 CIA/OCR/ADD/SD	2
1051 AFIT/LDE	1
P090 NSA/CDB	1
2206 FSL	1

Microfiche Nbr: FTD93C000537
FTD-ID(RS)T-0099-93